

Published in final edited form as:

J Cell Sci. 2007 March 15; 120(Pt 6): 973–984. doi:10.1242/jcs.03406.

Differential dynamics of Rab3A and Rab27A on secretory granules

Mark T W Handley, Lee P Haynes, and Robert D Burgoyne

The Physiological Laboratory School of Biomedical Sciences University of Liverpool Crown Street Liverpool L69 3BX

SUMMARY

We have assessed the dynamics of the association of Rab3A and Rab27A with secretory granules at various stages of their life in PC12 cells. Endogenous Rab3A colocalised with the secretory granule marker secretogranin II (SGII) and expressed EGFP-Rab3A and ECFP-Rab27A colocalised with one another. The extent of colocalisation between EGFP-Rab3A or EGFP-Rab27 and SGII increased after longer times post-transfection suggesting that these Rab proteins are preferentially recruited to newly synthesised granules. Following the release of immature secretory granules from the trans-Golgi network, Rab3A and Rab27A became associated with the immature granules after a lag period of around 20 minutes. Rab dynamics on granules were analysed in fluorescence recovery after photobleaching (FRAP) experiments. The recovery profile of EGFP-Rab27A was comparable to that of ppANF-EGFP, while the recovery profile of EGFP-Rab3A was significantly faster, indicating that Rab3A but not Rab27A may be rapidly exchanged between granules and cytosol. Inhibition of heat-shock protein 90 with 10 μ M geldanamycin did not affect the exchange process or regulated exocytosis. Rab dynamics during stimulation with 300 μ M ATP were analysed in live cells. Loss of granular ppANF-EGFP fluorescence was seen at the cell periphery after stimulation but only limited changes in EGFP-Rab3A and EGFP-Rab27A fluorescence was observed, indicating that the Rab proteins do not immediately dissociate or disperse on stimulation. The data suggest potentially distinct roles for Rab3A and Rab27A and we suggest that the finding that young secretory granules have a higher capacity for binding Rab3A and Rab27A may be functionally important for preferential exocytosis from these granules.

Keywords

Rab proteins; GTPases; Exocytosis; Secretion; secretory vesicle

INTRODUCTION

Rab proteins comprise the largest group within the Ras superfamily of monomeric GTPases, with 11 Rabs identified in yeast, and over 60 identified in mammals (Gurkan et al., 2005). Individual Rab subtypes characteristically associate with specific membrane compartments, and interact with specific effector(s) to regulate trafficking between compartments (Pereira-Leal and Seabra, 2000). The expansion of the Rab gene family in the higher eukaryotes is likely to reflect the increased complexity and regulation of membrane trafficking in these organisms, and particularly that associated with the specialisation of membrane trafficking pathways in specialised cell types (Bock et al., 2001). Regulated exocytosis is the release of vesicular or secretory granule contents in response to stimulation. A broad range of cell types including neuronal, exocrine, endocrine and immune cells are specialised for regulated

exocytosis, and there are sometimes dramatic differences in the regulation of the process and in the morphology of the organelles involved (Burgoyne and Morgan, 2003). It is thought that the core machinery of exocytosis, and indeed that of membrane fusion in general, is conserved in the form of the soluble N-ethyl maleimide-sensitive attachment protein receptor (SNARE) proteins, while many other proteins, including the Rabs and their effectors, are involved in adapting the process according to its discrete cellular or physiological roles.

Two groups of Rab proteins localised to vesicles and secretory granules, the isoforms of Rab3 and Rab27, have been directly implicated in regulated exocytosis, and much work has focused on the Rab3A and Rab27A isoforms. Rab3A overexpression is reported to be inhibitory (Holz et al., 1994; Johannes et al., 1998; Regazzi et al., 1996), although it may enhance constitutive exocytosis (Schluter et al., 2002). Rab27A overexpression is variously reported to inhibit or enhance regulated exocytosis (Desnos et al., 2003; Johnson et al., 2005; Menasche et al., 2003; Yi et al., 2002). Endogenous Rab3 and Rab27 isoforms, however, have positive roles in regulated exocytosis. Rab3A knockout mice show a moderate phenotype, with increased Ca^{2+} -triggered exocytosis leading to faster than normal 'rundown' of synaptic transmission in cultured hippocampal neurones (Geppert et al., 1994; Geppert et al., 1997), and reduced spontaneous neurotransmitter release at the neuromuscular synapse (Sons and Plomp, 2006). Mutation of Rab27A in humans results in Griscelli syndrome (Menasche et al., 2000) and loss of functional Rab27A in ashen mice is associated with defects in melanosome trafficking, defects in the exocytosis of lytic granules by cytotoxic T lymphocytes leading to immunodeficiency, and impaired release of insulin from pancreatic β -cells leading to glucose intolerance (Haddad et al., 2001; Kasai et al., 2005; Stinchcombe et al., 2004; Wilson et al., 2000). The importance of the Rab proteins in exocytosis may be even greater than the phenotypes of the mutant animals suggest if other Rab3 and Rab27 isoforms have roles that overlap with those of Rab3A and Rab27A, and partially compensate for their absence in the mutant animals. A quadruple knockout of Rab3A, Rab3B, Rab3C and Rab3D is post-natally lethal, and evoked exocytotic responses of cultured hippocampal neurones from these animals were reduced by ~30% compared to controls, a much greater effect than that seen when these isoforms were deleted singly (Schluter et al., 2004). A knock-in study in which mutant animals expressed EGFP-Rab27A on the native Rab27a promoter showed wider than expected expression of the protein in secretory endocrine and exocrine cells, and it is suggested that the most pronounced deficits in ashen mice are found in tissues that express only Rab27A (Tolmachova et al., 2004).

Like other small GTPases, Rabs are 'molecular switches', present in either GDP- or GTP-bound forms. When membrane-associated, they may become GTP-bound through interaction with specific guanine nucleotide exchange factors (GEFs). It is generally the GTP-bound form of the Rab that is considered active, and that interacts with effectors, though the Rab27 effector granuphilin-a/Slp4-a can interact with the GDP-bound Rab (Fukuda, 2003). Rabs hydrolyse bound GTP to GDP following interaction with specific GTPase-activating proteins (GAPs). In the GDP-bound form, Rabs may be vulnerable to extraction to the cytosol, a process involving guanine nucleotide dissociation inhibitor (GDIs) (Luan et al., 1999). GDIs stabilise the GDP-bound conformation of Rabs and are required for their cytosolic localisation, since all cytosolic Rab protein is GDI-bound. They are also thought to be important for correct targeting of Rabs back onto target membranes, a process also hypothesised to require a GDI displacement-factor (GDF) (Pfeffer, 2005). Standard models of Rab dynamics suggest a continuous cycle of organelle association and disassociation (Grosshans et al., 2006).

The regulation and dynamics of Rab3A in neurones have been partially characterised but less is known about Rab27A. Candidates for the Rab3GEP and Rab3GAP have been

described (Fukui et al., 1997; Nagano et al., 1998; Wada et al., 1996), and Rab3A is likely to associate with GDI α in preference to the other two GDI isoforms (Ishizaki et al., 2000). Rab3A on synaptic vesicles is largely GTP-bound, while GTP-hydrolysis has been linked to exocytosis (Stahl et al., 1994). Extraction of Rab3A from membranes is also suggested to be coupled to exocytosis as stimulation of neurons or synaptosomes was found to increase the proportion of the protein that was cytosolic (Fischer von Mollard et al., 1991; Sakisaka et al., 2002; Star et al., 2005). The extraction process is proposed to involve a GDI α -Hsp90 chaperone complex (GCC) comprising GDI α , the Hsp90/Hsc70 chaperone system, and the cysteine-string protein (CSP) (Sakisaka et al., 2002) and inhibition of Hsp90 has been shown to inhibit dissociation of Rab3A and exocytosis in brain synaptosomes. While it has been proposed that Rab3A cycles off membranes during or following exocytosis nothing is known about its constitutive recycling.

In the present study, we describe our findings regarding the regulation and dynamics of Rab3A and Rab27A in an endocrine secretory cell type, the PC12 cell. PC12 cells are a commonly used model endocrine cell line used in the study of exocytosis (Burgoyne and Morgan, 2003). Importantly, recent work has established that Rab3A and Rab27A are likely to be the only two Rabs that function in regulated exocytosis in this cell type and that both contribute in a non-redundant manner to secretory granule exocytosis (Tsuboi and Fukuda, 2006). Secretory granules are distributed throughout the cytosol in PC12 cells and have an approximately 10-fold larger diameter than synaptic vesicles (Warashina, 1985; Willig et al., 2006). It is therefore possible to resolve labelled secretory granules by conventional confocal microscopy and it is similarly practical to carry out fluorescence recovery after photobleaching (FRAP) experiments to investigate Rab dynamics directly on secretory granules. Secretory granules can exist in differing states during their life-cycle. After budding from the trans-Golgi network (TGN) immature granules move to the cell periphery where they are releasable but undergo maturation processes that result in an increase in their size, removal of specific components and their immobilisation in the cell cortex (Dittie et al., 1997; Rudolf et al., 2001; Tooze et al., 1991). Newly synthesised secretory granules (up to 16h old) undergo exocytosis in preference to older granules (Duncan et al., 2003). We have investigated the association of Rab3A and Rab27A with granules during various stages in their lifetime. We were able to demonstrate that Rab3A and Rab27A are recruited to immature granule shortly after budding and are associated preferentially with newly synthesised granules. In addition, Rab3A but not Rab27A is capable of exchanging rapidly between newly synthesised and older granules and cytosol but this exchange occurs in an HSP90-independent manner. Finally, neither Rab3A nor Rab27A disperses immediately when secretory granules undergo exocytosis.

METHODS

Plasmids

The rat Rab3A sequence was amplified from an existing vector (Haynes et al., 2001) by PCR and inserted into the pEGFP-C1 vector (Clontech, Basingstoke, UK) and the pmRFP-C1 vector (kind gift of RY Tsien) to generate mammalian expression constructs for Rab3A, N-terminally tagged with EGFP and monomeric red fluorescent protein (mRFP) (Campbell et al., 2002). Primers contained restriction endonuclease sites (underlined) to facilitate cloning. The sense primer used was 5'-AGCAGAAGCTTTAAATATGGCATCTGCCACAGACGCT-3'; *HindIII*, and the antisense primer was 5'-CAAGTATGGATCCGCTCAGCAGGCGCAGTCCTGATGCGG-3'; *BamHI*. PC12 cell cDNA was prepared from total PC12 cell RNA extracted using Trizol Reagent, (Invitrogen) followed by first strand cDNA synthesis with oligo dT(15) primers and Improm reverse transcriptase (Promega). The rat Rab27A sequence was amplified from the PC12 cDNA by

PCR and then inserted in frame into the pEGFP-C1, pECFP-C1 and pmRFP-C1 vectors to generate mammalian expression constructs for Rab27A, N-terminally tagged with EGFP, ECFP and mRFP. Primers contained restriction endonuclease sites (underlined) to facilitate subcloning. The sense primer used was 5'-AGCAGAAAGCTTTAAATATGTCGGATGGAGATTATGAC-3'; *HindIII*, and the antisense primer was 5'-CAAGTATGGATCCGCTCAACAGCCGCATAACCCCTTCTC-3'; *BamHI*. Sequences contained in the recombinant plasmids were verified by automated sequencing (DBS Genomics, Durham, UK) and comparison with published sequence information. The ppANF-EGFP (Burke et al., 1997), ARF1-EGFP (Haynes et al., 2005) and glucocorticoid receptor-EGFP (Galigniana et al., 1998) fusion constructs were as described previously. Human growth hormone (hGH) encoding plasmid (pXGH5) was obtained from Nichols Institute Diagnostics, San Clemente, USA.

Cell culture and transfection

PC12 cells were maintained in suspension in 75cm² culture flasks at 37°C in RPMI 1640 medium (Gibco, Paisley, UK) supplemented with 10% horse serum, 5% foetal calf serum, 100U/ml penicillin and 0.1mg/ml streptomycin. Transfection of PC12 cells was carried out as follows; 24-well plates were seeded with $\sim 4 \times 10^5$ cells per well on glass cover-slips and cells allowed to adhere overnight. Prior to transfection, the growth medium was replaced with 400 μ l/well Optimem 1 media (Gibco). Transfection mixes consisting of 3 μ l of Lipofectamine 2000 reagent (Invitrogen, Paisley, UK) per μ g plasmid in 100 μ l Optimem 1 media (Gibco) were prepared and incubated at room temperature for 20 min before being added dropwise to the cells. Five hours following their addition, transfection mixes were removed and replaced with normal growth medium.

Immunocytochemistry

Transfected cells grown on coverslips were washed in PBS and then fixed in 0.5ml 4% (v/v) paraformaldehyde for 30 min at room temperature. Coverslips were then washed twice in PBS, and exposed to primary antibody in PBS containing 0.3% BSA and 0.1% Triton-X-100 (PBT) for 1h. Primary antibodies, mouse anti-Rab3A (Transduction Labs, Cowley, UK), rabbit anti-secretogranin II (Abcam, Cambridge, UK), and rabbit anti-CSP (Chamberlain et al., 1996) were used at 1:400, 1:100 or 1:400 dilutions respectively. Unbound antibody was removed by washing three times with PBT, and coverslips were exposed to appropriate secondary antibodies at a 1:100 dilution in PBT for 1h. Either Alexa Fluor 488-conjugated, Alexa Fluor 594-conjugated (Molecular Probes, Paisley, UK), or biotinylated (Amersham Biosciences, Buckinghamshire, UK) secondary antibodies were used. After an additional round of washing, coverslips previously exposed to biotinylated antibody were exposed to a 1:50 dilution of streptavidin-conjugated Texas red (Amersham Biosciences) in PBT for 30 min. After a final washing step, coverslips were air dried prior to mounting on glass slides using Prolong antifade reagent (Molecular Probes).

Confocal microscopy

Confocal microscopy following immunocytochemistry was carried out on a Leica TCS-SP microscope (Leica Microsystems, Heidelberg, Germany) using a 63x oil immersion objective with a 1.4 numerical aperture and pinhole set to airy1. ECFP-containing constructs were excited using a 405nm laser, and emitted light was collected between 450-500nm. EGFP-containing constructs were excited using a 488nm laser and light collected between 500-550nm. Texas Red, Alexa Fluor 594 and monomeric red fluorescent protein were excited using a 594nm laser and light collected between 625-675nm. For the quantification of colocalization, images were analysed using the Manders Coefficient plug-in of ImageJ to generate values for the Pearson colocalization coefficient

Live cell confocal microscopy in bleaching and perfusion experiments was carried out on a Leica TCS-SP-MP microscope (Leica Microsystems) with images captured every 1.64s. A 63x water immersion objective with a 1.2 numerical aperture was used and the pinhole set to airy 2.06 (for photo-bleaching) or airy 3 for imaging before and after stimulation. For bleaching experiments, cells transfected with 0.5 μ g of each EGFP-containing construct were excited with a 488nm laser and light collected between 500-550nm. Bleaching was carried out by selecting circular regions of interest of diameter 2.5 μ m, using 75% of laser power. To determine the rate of fluorescence recovery, fluorescence in these regions was measured over time, and then normalised with respect to corresponding total cellular fluorescence at each individual time point to correct for bleaching during low power laser excitation. For perfusion experiments, cells were transfected with 0.1 μ g of each EGFP-containing construct. Transmitted light images were taken during experiments to ensure that changes in fluorescence were not a result of focal drift. All imaging of live cells and was carried out on cells at room temperature in Krebs Ringer buffer (NaCl 145mM, HEPES 20mM, Glucose 10mM, KCl 5mM, MgCl₂ 1.3mM, NaH₂PO₄ 1.2mM). Where the effects of geldanamycin (GA) were analysed, control cells were incubated in Krebs, and treated cells incubated in Krebs containing 10 μ M GA, for 1 hour prior to bleaching. For analysis of changes in intracellular Ca²⁺ concentration, cells were loaded with 5 μ M X-Rhod (Molecular Probes, Paisley) in 3mM Ca²⁺-Krebs for 20 minutes, and then in X-Rhod-free 3mM Ca²⁺-Krebs for a further 20 minutes prior to imaging. Where cells were stimulated, 300 μ M ATP in 3mM Ca²⁺-Krebs was applied by perfusion.

Assay of growth hormone secretion

Assay of exocytosis from transfected cells made use of heterologous expression of hGH expression (Wick et al., 1993) as described previously (Graham et al., 2000). In these experiments, 24-well poly-D-lysine-coated plates (BD Biosciences, San Jose, USA) were seeded with $\sim 4 \times 10^5$ cells per well, and cells were transfected as described. Each well was transfected with 0.5 μ g of the pXGH5 hGH-encoding vector either alone, or combined with other vectors as detailed in the text. 48 hours post transfection, cells were assayed for hGH release (Graham et al., 2000). Cells were washed once in 3mM Ca²⁺-Krebs, and then exposed to 200 μ l 3mM Ca²⁺-Krebs (unstimulated) or 200 μ l 3mM Ca²⁺-Krebs, 300 μ M ATP, (stimulated) for 15 minutes. hGH release (supernatant) was quantified using an enzyme-linked immunosorbent assay (ELISA) kit (Roche, East Sussex, UK) according to manufacturers' instructions. Levels of remaining cellular hGH were also quantified, to determine levels of total cellular hGH. The data for hGH secretion were calculated as a percentage of total hGH for each well and are presented as mean \pm SEM.

RESULTS

Exogenously expressed Rab3A and Rab27A are preferentially recruited to newly-synthesised secretory granules

In order to study the localisation and dynamics of Rab3A and Rab27A, expression vectors for N-terminally fluorescently-tagged versions of these proteins were generated. Coding sequences for the rat orthologues of the Rab proteins were amplified from an existing construct or rat PC12 cell cDNA respectively, and then sub-cloned into pEGFP-C1 or pEGFP-C1 expression vectors. It was decided to use N-terminally tagged constructs to avoid any potential deleterious effects on the C-terminal geranylgeranyl site of the Rabs that is required for membrane association. N-terminal modification does not appear to affect Rab protein function, as chimeric Rab27A, N-terminally tagged with GFP, has the capacity to functionally replace the wild-type protein in a mouse 'knock-in' model (Tolmachova et al., 2004).

Endogenous Rab3A and Rab27A are reported to associate with secretory granules in PC12 cells (Tsuboi and Fukuda, 2006). To confirm this localisation in PC12 cells, fixed cells were probed with antibodies against Rab3A, and the secretory granule marker protein secretogranin II (SGII) (Steiner et al., 1989). Fig. 1A-C shows that as expected, these proteins colocalise. It was not possible to carry out a similar experiment to determine the localisation of endogenous Rab27A because antibodies were not available. However, when ECFP-Rab27A and EGFP-Rab3A were coexpressed (Fig. 1D-F), their localisation was punctate, closely resembled that of endogenous Rab3A, and the two tagged Rab proteins showed punctate co-localisation. To determine whether the localisation of the exogenous Rab proteins matched that of the endogenous protein, cells were transfected with each of the constructs, fixed 18 hours post-transfection and then probed with the anti-SGII antibody. Surprisingly, the co-localisation between the exogenous Rabs and SGII was only partial (for an example, see the co-localisation between ECFP-Rab27A and SGII in Fig. 1G-I). Similar findings were made when cells were probed for cysteine string protein (CSP) (Fig 1J-L), another marker of secretory granules (Chamberlain et al., 1996). One possibility is that exogenously expressed Rabs become localised with only part of the cellular compliment of granules because the protein synthesised post-transfection was preferentially recruited to newly-synthesised secretory granules. To test this hypothesis, a transfectable granule content marker, prepro-atrial natriuretic factor-EGFP (ppANF-EGFP), was used. ppANF-EGFP is packaged within the granule core, and so can only label granules formed post-transfection (Burke et al., 1997). When it was cotransfected with ECFP-Rab27A (Fig. 1M-O), ppANF-EGFP showed almost complete co-localisation, suggesting that the Rab protein is recruited to the granules synthesised post-transfection as they mature, but is present to a lesser extent on older pre-existing secretory granules.

If the exogenous Rab proteins are recruited to granules during granule maturation, their co-localisation with SGII should improve over time as granules synthesised post-transfection make up a greater proportion of the total cellular compliment. To test this prediction, cells were transfected with EGFP-tagged Rab3A, Rab27A, or with ppANF-EGFP as a control, fixed at 18h and also at 30h post-transfection, probed with anti-SGII, and compared. Fig. 2 shows that co-localisation between each construct and SGII was partial after 18h but more extensive 30h after transfection and this was confirmed by quantitative analysis (Fig 2S). It seems therefore that the tagged Rab proteins are preferentially recruited to newly-synthesised secretory granules.

Association of Rab3A and Rab27A with immature secretory granules following their biogenesis

Studies in PC12 cells have shown that immature secretory granules move within seconds to the cell periphery following their budding from the TGN, and after a further period of 10s of minutes become immobilised in the cell cortex (Rudolf et al., 2001). During maturation secretory granules increase in size and specific components are removed from them with a half-time of around 45 mins (Dittie et al., 1997; Tooze et al., 1991). During the maturation period the granules can undergo regulated exocytosis (Tooze et al., 1991). We aimed to examine when it is during their biogenesis that the two Rab proteins become associated with secretory granules. To do this we made use of the blockade of vesicle formation at the TGN that is produced when cells are incubated at 20°C. This has been used previously to follow immature granules in PC12 cells (Rudolf et al., 2001). Following culture for 18h at 20°C, cells expressing ppANF-EGFP showed accumulated fluorescence in a perinuclear region, as expected if it was trapped in the TGN. Switching of the cells to 37°C for 30 mins resulted in extensive appearance of labelled punctate structures throughout the cells likely to be immature granules (Fig 3A). In contrast, expressed EGFP-tagged Rab3A and Rab27A showed a more diffuse cytosolic distribution at 20°C, although punctate structures were

visible indicating that a proportion of the Rabs can associate with some pre-existing granules. After 30 mins at 37°C, EGFP-Rab3A and EGFP-Rab27A were almost completely punctate in localisation suggesting that they had become associated with the immature granules. To follow the time course of their association with immature granules, cells were transfected to co-express ppANF-EGFP and Rab3A or Rab27A tagged with monomeric red fluorescent protein (Fig 3B). Immature secretory granules were visible throughout the cells after 5-10 mins following incubation at 37°C. Co-localisation of ppANF-EGFP and mRFP-Rab3A or mRFP-Rab27A was not evident, however, until the cells had been incubated at 37°C for 20 mins or more indicating a lag period between release of immature secretory granules from the TGN and the association of the Rab proteins of up to 20 min.

Rab3A but not Rab27A is dynamically associated with secretory granules in PC12 cells

Recruitment of Rab3A and Rab27A to newly-synthesised secretory granules is consistent with the suggestion made for synaptic vesicles that once the proteins associate with vesicles, they are only released during or following exocytosis (Fischer von Mollard et al., 1991; Star et al., 2005). In order to directly address this possibility, it was decided to employ fluorescence recovery after photobleaching (FRAP) experiments. In a FRAP experiment, the fluorescent protein within a small region of interest (ROI) of a cell is bleached using a high-intensity laser, and the recovery of fluorescence within this area is subsequently monitored (Lippincott-Schwartz and Patterson, 2003). The recorded fluorescence recovery reflects the replacement of bleached protein in the ROI with unbleached protein from outside this region. In order to test whether the protocol that was to be used could successfully resolve exchange of fluorescent protein between cytosol and membrane in PC12 cells, bleaching experiments were carried out on ARF1-EGFP-transfected cells. ARF1 is a small GTPase shown to cycle rapidly between cytosolic and Golgi complex-associated states in other cell types (Presley et al., 2002; Vasudevan et al., 1998). Expressed ARF-1-EGFP was partially cytosolic but also showed a clear localisation to a perinuclear region presumed to be the Golgi complex in PC12 cells (Fig 4A). Following the bleaching of an area of the Golgi complex, fluorescence recovery of this ARF-1-EGFP occurred with a $t_{1/2}$ of 44s and was almost complete (fractional recovery of 87.5%) within the recorded timeframe of the experiments (Fig 4A,E). This behaviour was similar to that described for ARF1 previously and confirms the applicability of the FRAP protocol in PC12 cells.

Following bleaching of fluorescently-tagged EGFP-Rab3A or EGFP-Rab27A, fluorescence recovery in the ROI could be attributed to three sources: the diffusion of unbleached cytosolic protein, exchange between bleached and unbleached protein on granule membranes, and the movement from other parts of the cell of granules carrying unbleached protein. Compared to the other components of recovery, diffusion of unbleached protein into the ROI was likely to be rapid (~ 1 s), while recovery due to granule movement was initially an unknown quantity. For the latter aspect, the recovery following bleaching of ppANF-EGFP was assessed (Fig. 4B, E and F). Since this protein is contained within granules, its recovery profile would be solely due to the effects of granule movement, and provides a reference for comparison with the other data. Imaging of live cells expressing ppANF-EGFP indicated that the labelled secretory granules had only limited mobility (see supplementary video). For photobleaching experiments, a small area of the cell was chosen containing several labelled secretory granules. Following photobleaching of ppANF-EGFP (Fig 4A, E and F) only a slow and partial recovery of fluorescence (fractional recovery of 23.7%) in the bleached region was observed with a $t_{1/2}$ of 58s consistent with limited secretory granule mobility under resting conditions in these cells.

EGFP-Rab27A or EGFP-RAB3A transfected cells were used in the FRAP experiments 18 hours post-transfection to analyse Rab dynamics on newly-synthesised granules and only cells expressing relatively low levels of the exogenous protein were selected. For Rab27A

(Fig 3C, E), as expected, it was found that proportionate fluorescence recovery at ~ 1.6 seconds post-bleaching (i.e. the first post-bleaching datapoint) was greater than seen in the ppANF-EGFP-transfected cells, consistent with a greater cytosolic component of recovery. However, when the data were normalised with respect to this initial datapoint, the recovery profiles of these proteins were not significantly different, suggesting that the minimal EGFP-Rab27A recovery seen after photobleaching was largely or entirely due to granule movement rather than exchange of Rab27A on the granules (Fig. 4F). In the case of EGFP-Rab3A (fractional recovery 66.6%), the recovery profile (Fig. 4D, E and F) was strikingly different to that of EGFP-Rab27A (fractional recovery 37.8%). The recovery of EGFP-Rab3A was more similar to that of the ARF1-EGFP with extensive although not complete recovery with a $t_{1/2}$ of 32s. These data suggest that like ARF1 but unlike Rab27A, Rab3A cycles continuously between cytosol and membranes, and that in PC12 cells at least, this recycling is not exclusively coupled to the exocytotic event.

The apparent difference between newly synthesised and pre-existing secretory granules in terms of the amount of tagged Rab3A that becomes associated to give differing fluorescence intensities at 18h post-transfection and more homogenous intensity after 30h post-transfection could have two explanations. The first is that Rab3A on older granules is unable to cycle between the granules and cytosol. The second is that the capacity of old granules for recruitment of Rab3A is lower than that of newer granules. To test the possibility of a difference in cycling we carried out FRAP experiments on older EGFP-Rab3A-labelled granules in cells at 30 and 54h after transfection and compared these to granules in cells at 18h post-transfection. As shown in Fig 5 EGFP-Rab3A recovered with similar kinetics onto granules in cells at 18, 30 and 54h but with a slightly higher fractional recovery for the older granules. These data indicate that Rab3A can cycle on and off both newly synthesised and older granules.

In PC12 cells, inhibition of HSP90 does not affect Rab3A dynamics or regulated exocytosis

Recent work has suggested that Rab protein extraction from membranes involves the heat-shock protein Hsp90 (Chen and Balch, 2006; Sakisaka et al., 2002). More specifically, it was previously found that extraction of Rab3A from synaptosome membranes was regulated by a chaperone complex containing GDI α , Hsp90, Hsc70 and CSP (Sakisaka et al., 2002) and also that inhibition of Hsp90 inhibited calcium-triggered exocytosis in synaptosomes. While the authors suggest that Hsp90-dependent Rab3A extraction is coupled to exocytosis, it was possible that the continuous cycling of EGFP-Rab3A between membrane and cytosol that we observed was also mediated via this complex. In order to investigate this possibility, parallel bleaching experiments were carried out on control EGFP-Rab3A-transfected cells, and cells incubated with 10 μ M geldanamycin for 1 hour prior to bleaching. Geldanamycin is a potent and specific inhibitor of Hsp90, and was used here at the concentration found to virtually abolish extraction of Rab3A from synaptosomal membranes (Sakisaka et al., 2002) following stimulation with Ca²⁺. The recovery profile for EGFP-Rab3A following photobleaching in control cells was closely similar to that in the earlier experiments (compare Fig 4 and 6). It was found that recovery profiles for control and treated cells were virtually identical (Fig. 6A) with a $t_{1/2}$ of 29 and 28.6s for control and geldanamycin treated cells respectively suggesting that the observed EGFP-Rab3A cycling occurs independently of Hsp90. It was also reported that geldanamycin could block neurotransmitter release from synaptosomes. In order to see whether there was a similar effect on the release of secretory granule contents from PC12 cells, we assayed ATP-stimulated release of exogenously-expressed human growth hormone (hGH) from PC12 cells pre-incubated for 1h prior to stimulation with varying concentrations of the inhibitor (see Fig. 6B). The release of hGH was assayed as this would allow examination of release from newly synthesised granules in transfected cells (i.e. those that exogenous Rabs become associated with). As shown,

geldanamycin had no significant effect on hGH release within the range of concentrations used suggesting that secretory granule exocytosis occurs in an Hsp90-independent manner in this cell type.

It was possible that the negative results described above were caused because the geldanamycin used was inactive, or because PC12 cells were in some way resistant to its effects. To rule out these possibilities, the effects of the inhibitor on the well characterised Hsp90-dependent nuclear translocation of glucocorticoid receptor (GCR) were determined. It has been found that 10 μ M geldanamycin can block dexamethasone-induced nuclear translocation of GCR-EGFP in NIH-3T3 cells (Galigniana et al., 1998), and so this protocol was applied to PC12 cells. GCR-EGFP-transfected cells were serum-starved, chilled on ice, exposed to 1 μ M dexamethasone, and then either vehicle or 10 μ M geldanamycin. Following a brief period of incubation at 37°C and fixation, 100 cells per treatment expressing moderate amounts of this protein were scored according to its localisation. In individual cells in the cultures the GCR-EGFP was either predominantly in the cytosol or nucleus (Fig. 6C). As expected, the presence of geldanamycin increased the proportion of cells in which the CGR-EGFP was cytosolic (Fig 6D), indicating that it was indeed active in PC12 cells.

Exocytosis of secretory granules in PC12 cells does not lead to immediate dispersal of Rab3A and Rab27A to the cytosol

It has previously been reported that activation of exocytosis leads to Rab3A extraction from synaptic membranes (Fischer von Mollard et al., 1991; Star et al., 2005). Indeed, Star et al. have directly imaged the reversible dispersal of EGFP-Rab3A away from presynaptic terminals and into neighbouring axonal regions during periods of synaptic activity. It is unknown, however, whether dissociation and dispersal occurs for Rabs located on dense core secretory granules. In addition, experiments on synaptic Rabs requires use of either biochemical approaches or imaging of whole synaptic terminals whereas study of PC12 cells allows imaging of events on single secretory granules in live cells. Therefore, it was decided to image EGFP-Rab3A and EGFP-Rab27A-transfected cells during stimulation with ATP to raise intracellular calcium and activate exocytosis in PC12 cells. As it has been reported that over-expression of Rab3A or Rab27A in PC12 cells inhibits secretion (Chung et al., 1999; Desnos et al., 2003; Schluter et al., 2002), it was first necessary to make sure that transfected cells were capable of exocytosis. Cells were co-transfected with a range of concentrations of each Rab expression vector and an expression vector encoding human growth hormone. At 48 hours post-transfection, cells were stimulated with 300 μ M ATP and secreted hGH was assayed. Transfection with high levels of EGFP-Rab3A or EGFP-Rab27A plasmids substantially inhibited evoked exocytosis of hGH and plasmids encoding untagged Rabs had a similar effect. At lower levels of plasmid (0.05 or 0.1 μ g), however, exocytosis was only partially reduced (data not shown) indicating that the imaging experiments could be carried out.

Live cell imaging experiments were continued using low plasmid concentrations. In addition, cells transfected with 0.1 μ g of each plasmid were imaged at only 18 hours post-transfection so that expression levels of the Rabs would be less than in the 48h hGH experiments and only those cells expressing low levels of fluorescence were monitored. Cells were loaded with the Ca²⁺ indicator X-Rhod for measurement of changes in intracellular Ca²⁺ concentration resulting from stimulation to confirm that the cells responded to 300 μ M ATP. An increase in Ca²⁺ concentration was found to occur in all cells analysed and the mean change in X-Rhod fluorescence over the time course of experiments is shown in Fig. 7A. Images were taken using settings to image within a thick confocal section to ensure that granules were not lost due to movement out of the confocal section and cells were rejected if any focus drift due to cell movement was detected. Initially, ppANF-EGFP-transfected cells were observed to see if the cells underwent exocytosis in

response to 300 μ M ATP (Fig. 7B,C). As noted above there is little movement or loss of granules from the imaged field under resting conditions. During stimulation, ppANF-labelled granules in the cell periphery but not those in the cell interior were seen to disappear abruptly often between successive images (Fig 7B), indicating exocytosis of these granules. The number of granules lost per cell was variable but on average close to 20% of labelled granules (9 per cell, Fig 7C) disappeared. This can be seen in the example shown in Figure 7C in which images before (green) and after (red) stimulation have been overlaid so that granules that remained are seen as yellow. In contrast, when EGFP-Rab3A or EGFP-Rab27A-transfected cells were imaged during stimulation, while some short-range granule movement was noted, there was no overall loss of fluorescent granules at the cell periphery or in the cell interior (see Fig. 7C). These results suggest that dissociation of Rab3A and Rab27A from secretory granules does not occur following stimulation nor do the Rabs immediately disperse from the sites of exocytosis at the plasma membrane in PC12 cells.

DISCUSSION

We have examined various aspects of the dynamics and lifecycle of Rab3A and Rab27A on secretory granules in PC12 cells. Four lines of evidence from the data presented here point to the suggestion that on exogenous expression Rabs 3A and 27A are recruited preferentially to newly synthesised granules in PC12 cells: the initially partial co-localisation of the exogenous Rab proteins with SGII; their stronger co-localisation with ppANF-EGFP; their stronger co-localisation with SGII over time post transfection; their more diffuse cytosolic localisation in cells in which budding of new granules from the TGN has been blocked. Under conditions where formation of new granules is blocked, more of the Rab3A and Rab27A were cytosolic but some was associated with pre-existing granules indicating that the exogenously expressed Rabs can associate to a lesser extent with older granules. The 20 °C block experiments also demonstrate that Rab3A and Rab27A only become associated with immature secretory granules after a lag period of 10-20 min following budding from the TGN. At this time immature secretory granules in PC12 cells can undergo regulated exocytosis (Tooze et al., 1991).

The data from FRAP analysis showed that Rab3A, but not Rab27A can cycle rapidly between the granule membrane and the cytosol. The reproducibility of the Rab3A cycling data was shown by the independent series of experiments carried out including those in the presence or absence of gelanamycin. The findings for Rab3A are not unexpected as other small GTPases (Mochizuki et al., 2001; Presley et al., 2002; Vasudevan et al., 1998), and indeed Rab5 and Rab7 have shown similar properties. FRAP experiments on EGFP-Rab5 exogenously expressed in CHO cells showed that the bleached protein on phagosomes is rapidly replaced with a $t_{1/2}$ of ~5 seconds (Vieira et al., 2003). EGFP-Rab7 expressed in Mel JuSo cells is replaced on endosomes and lysosomes with a $t_{1/2}$ of ~52 seconds, while 31% of the protein was found to be in an immobile fraction (Jordens et al., 2001) The finding that in contrast, Rab27A does not cycle once it becomes granule associated is surprising and differs from other Rabs that have been examined but is consistent with other recent data showing that in unstimulated platelets Rab27A is predominantly in a GTP-bound and membrane-associated form (Kondo et al., 2006) whereas in the case of Rab3A in synaptosomes there is a significant cytosolic GDP-bound pool (Stahl et al., 1994).

How can the preferential recruitment of Rab3A to newly synthesised granules be explained? One possibility is that this is due to differences in the exchangeability of Rab3A between new and old granules and that while that Rab3A can initially cycle between these and the cytosol, over time, it becomes progressively more tightly associated and unexchangeable as the granules age. Perhaps Rab3A becomes segregated to a stable multimolecular 'rab domain' such as that reported for Rab5 and Rab9 (Ganley et al., 2004; Zerial and McBride,

2001), and this domain is resistant to disassembly due to positive feedback activation of Rab GEF. Alternatively, it could be suggested that sites for tight binding between Rab protein and granule membrane are saturable and that the capacity of older granules for binding Rab3 is lower than younger granules. The finding that EGFP-Rab3A could cycle between cytosol and newly synthesis (18h) or older (30 and 54h) granules in FRAP experiments provides an important clue that supports the latter explanation.

What is the explanation for the striking difference between Rab3A and Rab27A dynamics? Both Rab3A and Rab27A are likely to be targeted to saturable binding sites on newly synthesised granules. What is the mechanistic basis for the observed difference between Rab3A and Rab27A? A simple explanation for this difference might be that on granules, Rab3A has a higher intrinsic GTP hydrolysis rate than Rab27A, with cycling dependent on the presence of releasable GDP-bound Rab protein. Another possibility would be differential regulation by Rab-specific GAPs. Rab3GAP is present on synaptic vesicles, and may be active here and also on secretory granules (Sakane et al., 2006) and a distinct candidate Rab27 GAP has been described recently (Itoh and Fukuda, 2006). Another possibility is that GTP-bound Rab27A is unable to dissociate from membranes once it is bound. This would be consistent with data showing that Rab27A has a low intrinsic GTPase activity and also that the GDP-bound form of Rab27A in platelets remains membrane-associated in stimulated cells (Kondo et al., 2006). The differential dynamics of Rab3A and Rab27A on secretory granules suggests that these two Rabs may have distinct functional roles in exocytosis and this would be consistent with differences in effectors preferred by these Rabs (Fukuda, 2005) and the finding that they appear to act in concert on granule docking (Tsuboi and Fukuda, 2006).

One already identified mechanism of Rab3A extraction into the cytosol is that involving an Hsp90-containing complex (Sakisaka et al., 2002). However, we found that Hsp90 inhibition by geldanamycin had no effect on Rab3A cycling as identified by FRAP nor did it affect exocytosis. The concentration of the inhibitor used was sufficient to inhibit dexamethasone-induced nuclear translocation of GCR-EGFP. One interpretation of the data is that the mechanism for membrane-extraction of Rab3A differs between PC12 cells and neurones. However, (Chen and Balch, 2006) reported that an Hsp90-dependent mechanism of Rab extraction operates on other Rab subtypes and in various cell types making this interpretation unlikely. Another interpretation is that separate mechanisms exist for Rab-extraction during rapid cycling, and Rab-extraction where a donor membrane compartment meets its target membrane. Under this interpretation the Hsp90-dependent mechanism would control only Rab-extraction at the target membrane. Removal of the Rab during cycling may involve the removal of the Rab alone, while removal of the Rab at the target membrane is likely to require the disassembly of Rab-containing complexes. It should be noted, however, that unlike the situation in synaptosomes (Sakisaka et al., 2002), geldanamycin had no detectable effect on exocytosis in PC12 cells.

Previous studies on Rab3A have identified neuronal Rab3A dissociation and dispersal coupled to exocytosis (Fischer von Mollard et al., 1991; Sakisaka et al., 2002; Star et al., 2005). In contrast, one study on Rab3A in synaptosomes observed that after stimulation GDP-loaded Rab3A remained membrane-associated (Stahl et al., 1994). We found that in stimulated PC12 cells secretory granule-associated Rab3A and Rab27A did not dissociate from granules nor disperse when cells were stimulated. Evidence has been provided for very rapid retrieval of dense-core granules (Graham et al., 2002; Holroyd et al., 2002). It is possible, therefore, that Rab3A and Rab27A in PC12 cells remain clustered at the plasma membrane following exocytosis in a manner similar to synaptotagmin in neurones (Willig et al., 2006). In PC12 cells, the functional requirement for the Rab, or the scale of the dispersal process, may differ in this regard to that in neurones. Nevertheless, the findings reported

here suggest that the dissociation of Rab3A and Rab27A from membranes is not an integral aspect of the exocytotic process. In addition, the stable association of Rab3A and Rab27A with secretory granules would be consistent with a role for these Rabs in maintaining the fusion competency of secretory vesicles and perhaps the differing dynamics of these two Rabs may underlie the dual requirement for them in dense-core granule exocytosis (Tsuboi and Fukuda, 2006).

Recent work by Schluter et al. has improved understanding of the function of Rab3A in synaptic exocytosis and suggested that Rab3A boosts the release probability of a subset of the vesicles of the readily-releasable pool. This finding presents the question as to how Rab3A, which is present on all vesicles, can regulate the properties of only some. It may be relevant that in chromaffin cells, one factor regulating the release probability of secretory granules is granule age, with newly synthesised granules reportedly released in preference to older granules (Duncan et al., 2003). The molecular basis for this difference between old and young granules has been unknown. Since we describe data suggesting that Rab3A and Rab27A associate preferentially with young granules, it is an intriguing possibility that this is a functionally important determinant of this phenomenon.

Acknowledgments

MTWH was supported by an MRC DTA Research Studentship and work in this laboratory was also supported by a Wellcome Trust Programme grant to RDB. The authors thank Prof Alexei Tepikin for providing access to confocal microscopes and for his advice and Prof R Tsien for the monomeric red fluorescent protein construct.

REFERENCES

- Bock JB, Matern HT, Peden AA, Scheller RH. A genomic perspective on membrane compartment organisation. *Nature*. 2001; 409:839–841. [PubMed: 11237004]
- Burgoyne RD, Morgan A. Secretory granule exocytosis. *Physiol. Rev.* 2003; 83:581–632. [PubMed: 12663867]
- Burke NV, Han W, Li D, Takimoto K, Watkins SC, Levitan ES. Neuronal peptide release is limited by secretory granule mobility. *Neuron*. 1997; 19:1095–102. [PubMed: 9390522]
- Campbell RE, Tour O, Palmer AE, Steinbach PA, Baird GS, Zacharias DA, Tsien RY. A monomeric red fluorescent protein. *Proc Natl Acad Sci U S A*. 2002; 99:7877–82. [PubMed: 12060735]
- Chamberlain LH, Henry J, Burgoyne RD. Cysteine string proteins are associated with chromaffin granules. *J. Biol.Chem.* 1996; 271:19514–19517. [PubMed: 8702643]
- Chen CY, Balch WE. The Hsp90 Chaperone Complex Regulates GDI-dependent Rab Recycling. *Mol Biol Cell*. 2006; 17:3494–507. [PubMed: 16687576]
- Chung S-H, Joberty G, Gelino EA, Macara IG, Holz RW. Comparison of the effects on secretion in chromaffin and PC12 cells of Rab3 family members and mutants. *J.Biol.Chem.* 1999; 274:18113–18120. [PubMed: 10364266]
- Desnos C, Schonn JS, Huet S, Tran VS, El-Amraoui A, Raposo G, Fanget I, Chapuis C, Menasche G, de Saint Basile G, et al. Rab27A and its effector MyRIP link secretory granules to F-actin and control their motion towards release sites. *J Cell Biol*. 2003; 163:559–70. [PubMed: 14610058]
- Dittie AS, Thomas L, Thomas G, Tooze SA. Interaction of furin in immature secretory granules from neuroendocrine cells with the AP-1 adaptor complex is modulated by casein kinase II phosphorylation. *Embo J*. 1997; 16:4859–70. [PubMed: 9305628]
- Duncan RR, Greaves J, Wiegand UK, Matskevich I, Bodammer G, Apps DK, Shipston MJ, Chow RH. Functional and spatial segregation of secretory vesicle pools according to vesicle age. *Nature*. 2003; 422:176–180. [PubMed: 12634788]
- Fischer von Mollard G, Sudhof TC, Jahn R. A small GTP-binding protein dissociates from synaptic vesicles during exocytosis. *Nature*. 1991; 349:79–81. [PubMed: 1845915]

- Fukuda M. Slp4-a/granuphilin-a inhibits dense-core vesicle exocytosis through interaction with the GDP-bound form of Rab27a in PC12 cells. *J. Biol. Chem.* 2003; 278:15390–15396. [PubMed: 12590134]
- Fukuda M. Versatile role of rab27 in membrane trafficking: Focus on the rab27 effector families. *J. Biochem.* 2005; 137:9–16. [PubMed: 15713878]
- Fukui K, Sasaki T, Imazumi K, Matsuura Y, Nakanishi H, Takai Y. Isolation and characterization of a GTPase activating protein specific for the Rab3 subfamily of small G proteins. *J Biol Chem.* 1997; 272:4655–8. [PubMed: 9030515]
- Galigiana MD, Scruggs JL, Herrington J, Welsh MJ, Carter-Su C, Housley PR, Pratt WB. Heat shock protein 90-dependent (geldanamycin-inhibited) movement of the glucocorticoid receptor through the cytoplasm to the nucleus requires intact cytoskeleton. *Mol Endocrinol.* 1998; 12:1903–13. [PubMed: 9849964]
- Ganley IG, Carroll K, Bittova L, Pfeffer S. Rab9 GTPase regulates late endosome size and requires effector interaction for its stability. *Mol Biol Cell.* 2004; 15:5420–30. [PubMed: 15456905]
- Geppert M, Bolshakov VY, Siegelbaum SA, Takei K, De Camilli P, Hammer RE, Sudhof TC. The role of Rab3A in neurotransmitter release. *Nature.* 1994; 369:493–497. [PubMed: 7911226]
- Geppert M, Goda Y, Stevens CF, Sudhof TC. The small GTP-binding protein rab3a regulates a late step in synaptic vesicle fusion. *Nature.* 1997; 387:810–814. [PubMed: 9194562]
- Graham ME, Fisher RJ, Burgoyne RD. Measurement of exocytosis by amperometry in adrenal chromaffin cells: effects of clostridial neurotoxins and activation of protein kinase C on fusion pore kinetics. *Biochimie.* 2000; 82:469–479. [PubMed: 10865133]
- Graham ME, O'Callaghan DW, McMahon HT, Burgoyne RD. Dynamin-dependent and dynamin-independent processes contribute to the regulation of single vesicle release kinetics and quantal size. *Proc. Natl. Acad. Sci. USA.* 2002; 99:7124–7129. [PubMed: 11997474]
- Grosshans BL, Ortiz D, Novick P. Rabs and their effectors: achieving specificity in membrane traffic. *Proc Natl Acad Sci U S A.* 2006; 103:11821–7. [PubMed: 16882731]
- Gurkan C, Lapp H, Alory C, Su AI, Hogenesch JB, Balch WE. Large-scale profiling of Rab GTPase trafficking networks: the membrome. *Mol Biol Cell.* 2005; 16:3847–64. [PubMed: 15944222]
- Haddad EK, Wu XF, Hammer JA, Henkart PA. Defective granule exocytosis in Rab27a-deficient lymphocytes from Ashen mice. *J. Cell Biol.* 2001; 152:835–841. [PubMed: 11266473]
- Haynes LP, Evans GJO, Morgan A, Burgoyne RD. A direct inhibitory role for the Rab3 specific effector, Noc2, in Ca²⁺-regulated exocytosis in neuroendocrine cells. *J. Biol. Chem.* 2001; 276:9726–9732. [PubMed: 11134008]
- Haynes LP, Thomas GMH, Burgoyne RD. Interaction of neuronal calcium sensor-1 and ARF1 allows bidirectional control of PI(4) kinase and TGN-plasma membrane traffic. *J. Biol. Chem.* 2005; 280:6047–6054. [PubMed: 15576365]
- Holroyd P, Lang T, Wenzel D, Decamilli P, Jahn R. Imaging direct, dynamin-dependent recapture of fusing secretory granules on plasma membrane lawns from PC12 cells. *Proc. Natl. Acad. Sci.* 2002; 99:16806–16811. [PubMed: 12486251]
- Holz RW, Brondyk WH, Senter RA, Kuizon L, Macara IG. Evidence for the involvement of Rab3A in Ca²⁺-dependent exocytosis from adrenal chromaffin cells. *J. Biol. Chem.* 1994; 269:10229–10234. [PubMed: 8144603]
- Ishizaki H, Miyoshi J, Kamiya H, Togawa A, Tanaka M, Sasaki T, Endo K, Mizoguchi A, Ozawa S, Takai Y. Role of rab GDP dissociation inhibitor alpha in regulating plasticity of hippocampal neurotransmission. *Proc Natl Acad Sci U S A.* 2000; 97:11587–92. [PubMed: 11027356]
- Itoh T, Fukuda M. Identification of EPI64 as a GTPase-activating protein specific for Rab27A. *J Biol Chem.* 2006
- Johannes L, Lledo PM, Chameau P, Vincent JD, Henry JP, Darchen F. Regulation of the Ca²⁺ sensitivity of exocytosis by Rab3a. *J Neurochem.* 1998; 71:1127–33. [PubMed: 9721737]
- Johnson JL, Ellis BA, Noack D, Seabra MC, Catz SD. The Rab27a-binding protein, JFC1, regulates androgen-dependent secretion of prostate-specific antigen and prostatic-specific acid phosphatase. *Biochem J.* 2005; 391:699–710. [PubMed: 16004602]

- Jordens I, Fernandez-Borja M, Marsman M, Dusseljee S, Janssen L, Calafat J, Janssen H, Wubbolts R, Neefjes J. The Rab7 effector protein RILP controls lysosomal transport by inducing the recruitment of dynein-dynactin motors. *Curr. Biol.* 2001; 11:1680–1685. [PubMed: 11696325]
- Kasai K, Ohara-Imaizumi M, Takashi N, Mizutani S, Zhao S, Kikuta T, Kasai H, Nagamatsu S, Gomi H, Izumi T. Rab27a mediates the tight docking of insulin granules onto the plasma membrane during glucose stimulation. *J. Clin. Invest.* 2005; 115:388–396. [PubMed: 15690086]
- Kondo H, Shirakawa R, Higashi T, Kawato M, Fukuda M, Kita T, Horiuchi H. Constitutive GDP/GTP exchange and secretion-dependent GTP hydrolysis activity for Rab27 in platelets. *J Biol Chem.* 2006
- Lippincott-Schwartz J, Patterson GH. Development and use of fluorescent protein markers in living cells. *Science.* 2003; 300:87–91. [PubMed: 12677058]
- Luan P, Balch WE, Emr SD, Burd CG. Molecular dissection of guanine nucleotide dissociation inhibitor function *in vivo*. Rab-independent binding to membranes and role of Rab recycling factors. *J Biol Chem.* 1999; 274:14806–17. [PubMed: 10329679]
- Menasche G, Feldmann J, Houdusse A, Desaymard C, Fischer A, Goud B, de Saint Basile G. Biochemical and functional characterization of Rab27a mutations occurring in Griscelli syndrome patients. *Blood.* 2003; 101:2736–42. [PubMed: 12446441]
- Menasche G, Pastural E, Feldmann J, Certain S, Ersoy F, Dupuis S, Wulffraat N, Bianchi D, Fischer A, Le Deist F, et al. Mutations in RAB27A cause Griscelli syndrome associated with haemophagocytic syndrome. *Nature Genetics.* 2000; 25:173–176. [PubMed: 10835631]
- Mochizuki N, Yamashita S, Kurokawa K, Ohba Y, Nagai T, Miyawaki A, Matsuda M. Spatio-temporal images of growth-factor-induced activation of Ras and Rap1. *Nature.* 2001; 411:1065–8. [PubMed: 11429608]
- Nagano F, Sasaki T, Fukui K, Asakura T, Imazumi K, Takai Y. Molecular cloning and characterization of the noncatalytic subunit of the Rab3 subfamily-specific GTPase-activating protein. *J Biol Chem.* 1998; 273:24781–5. [PubMed: 9733780]
- Pereira-Leal JB, Seabra MC. The mammalian Rab family of small GTPases: definition of family and subfamily sequence motifs suggests a mechanism for functional specificity in the Ras superfamily. *J Mol Biol.* 2000; 301:1077–87. [PubMed: 10966806]
- Pfeffer S. A model for Rab GTPase localization. *Biochem Soc Trans.* 2005; 33:627–30. [PubMed: 16042559]
- Presley JF, W TH, Pfeifer AC, Siggia ED, Phair RD, Lippincott-Schwartz J. Dissection of COPI and Arf1 dynamics *in vivo* and role in Golgi membrane transport. *Nature.* 2002; 417:187–193. [PubMed: 12000962]
- Regazzi R, Ravazzola M, Iezzi M, Lang J, Zahraoui A, Anderegg E, Morel P, Takai Y, Wollheim CB. Expression, localisation and functional role of small GTPases of the Rab3 family in insulin-secreting cells. *J.Cell Sci.* 1996; 109:2265–2273. [PubMed: 8886977]
- Rudolf R, Salm T, Rustom A, Gerdes HH. Dynamics of immature secretory granules: role of cytoskeletal elements during transport, cortical restriction, and F-actin-dependent tethering. *Mol Biol Cell.* 2001; 12:1353–65. [PubMed: 11359927]
- Sakane A, Manabe S, Ishizaki H, Tanaka-Okamoto M, Kiyokage E, Toida K, Yoshida T, Miyoshi J, Kamiya H, Takai Y, et al. Rab3 GTPase-activating protein regulates synaptic transmission and plasticity through the inactivation of Rab3. *Proc Natl Acad Sci U S A.* 2006; 103:10029–34. [PubMed: 16782817]
- Sakisaka T, Meerlo T, Matteson J, Plutner H, Balch WE. Rab-αGDI activity is regulated by a Hsp90 chaperone complex. *EMBO J.* 2002; 21:6125–6135. [PubMed: 12426384]
- Schluter OM, Khvotchev M, Jahn R, Sudhof TC. Localisation versus function of rab3 proteins. *J.Biol. Chem.* 2002; 277:40919–40929. [PubMed: 12167638]
- Schluter OM, Schmitz F, Jahn R, Rosenmund C, Sudhof TC. A complete genetic analysis of neuronal rab3 function. *J. Neurosci.* 2004; 24:6629–6637. [PubMed: 15269275]
- Sons MS, Plomp JJ. Rab3A deletion selectively reduces spontaneous neurotransmitter release at the mouse neuromuscular synapse. *Brain Res.* 2006; 1089:126–134. [PubMed: 16631140]

- Stahl B, von Mollard GF, Walch-Solimena C, Jahn R. GTP cleavage by the small GTP-binding protein Rab3A is associated with exocytosis of synaptic vesicles induced by alpha-latrotoxin. *J Biol Chem.* 1994; 269:24770–6. [PubMed: 7929154]
- Star EN, Newton AJ, Murthy VN. Real-time imaging of Rab3a and Rab5a reveals differential roles in presynaptic function. *J. Physiol.* 2005; 569:103–117. [PubMed: 16141272]
- Steiner HJ, Schmid KW, Fischer-Colbrie R, Sperk G, Winkler H. Co-localization of chromogranin A and B, secretogranin II and neuropeptide Y in chromaffin granules of rat adrenal medulla studied by electron microscopic immunocytochemistry. *Histochemistry.* 1989; 91:473–7. [PubMed: 2475463]
- Stinchcombe J, Bossi G, Griffiths GM. Linking albinism and immunity: the secrets of secretory lysosomes. *Science.* 2004; 305:55–9. [PubMed: 15232098]
- Tolmachova T, Anders R, Stinchcombe JC, Bossi G, Griffiths GM, Huxley C, Seabra MC. A general role for Rab 27a in secretory cells. *Mol. Biol. Cell.* 2004; 15:332–344. [PubMed: 14617806]
- Tooze SA, Flatmark T, Tooze J, Huttner WB. Characterization of the immature secretory granule, an intermediate in granule biogenesis. *J. Cell Biol.* 1991; 115:1491–1503. [PubMed: 1757459]
- Tsuboi T, Fukuda M. Rab3A and Rab27A cooperatively regulate the docking step of dense-core vesicle exocytosis in PC12 cells. *J Cell Sci.* 2006; 119:2196–203. [PubMed: 16684812]
- Vasudevan C, Han W, Tan Y, Nie Y, Li D, Shome K, Watkins SC, Levitan ES, Romero G. The distribution and translocation of the G protein ADP-ribosylation factor 1 in live cells is determined by its GTPase activity. *J Cell Sci.* 1998; 111(Pt 9):1277–85. [PubMed: 9547306]
- Vieira OV, Bucci C, Harrison RE, Trimble WS, Lanzetti L, Gruenberg J, Schreiber AD, Stahl B, Grinstein S. Modulation of Rab5 and Rab7 recruitment to phagosomes by phosphatidylinositol 3-kinase. *Mol. Cell. Biol.* 2003; 23:2501–2514. [PubMed: 12640132]
- Wada M, Nakanishi H, Satoh A, Hirano H, Obashi H, Matsuura Y, Takai Y. Isolation and Characterisation of a GDP/GTP Exchange Protein Specific for the Rab3 Subfamily Small G Proteins. *J. Biol. Chem.* 1996; 272:3875–3878. [PubMed: 9020086]
- Warashina A. Changes in the size of isolated chromaffin granules in ATP-evoked catecholamine release. *FEBS Lett.* 1985; 184:87–9. [PubMed: 3987907]
- Wick PF, Senter RA, Parsels LA, Uhler MD, Holz RW. Transient transfection studies of secretion in bovine chromaffin cells and PC12 cells. Generation of kainate-sensitive chromaffin cells. *J. Biol. Chem.* 1993; 268:10983–10989. [PubMed: 8496162]
- Willig KI, Rizzoli SO, Westphal V, Jahn R, Hell SW. STED microscopy reveals that synaptotagmin remains clustered after synaptic vesicle exocytosis. *Nature.* 2006; 440:935–9. [PubMed: 16612384]
- Wilson SM, Yip R, Swing DA, O'Sullivan TN, Zhang Y, Novak EK, Swank RT, Russell LB, Copeland NG, Jenkins NA. A mutation in Rab27a causes the vesicle transport defects observed in ashen mice. *Proc. Natl. Acad. Sci. U.S.A.* 2000; 97:7933–7938. [PubMed: 10859366]
- Yi Z, Yokota H, Torii S, Aoki T, Hosaka M, Zhao S, Takata K, Takeuchi T, Izumi T. The Rab27a/granuphilin complex regulates the exocytosis of insulin-containing dense-core granules. *Mol. Cell. Biol.* 2002; 22:1858–1867. [PubMed: 11865063]
- Zerial M, McBride H. Rab proteins as membrane organizers. *Nature Reviews Molecular Cell Biology.* 2001; 2:107–117.

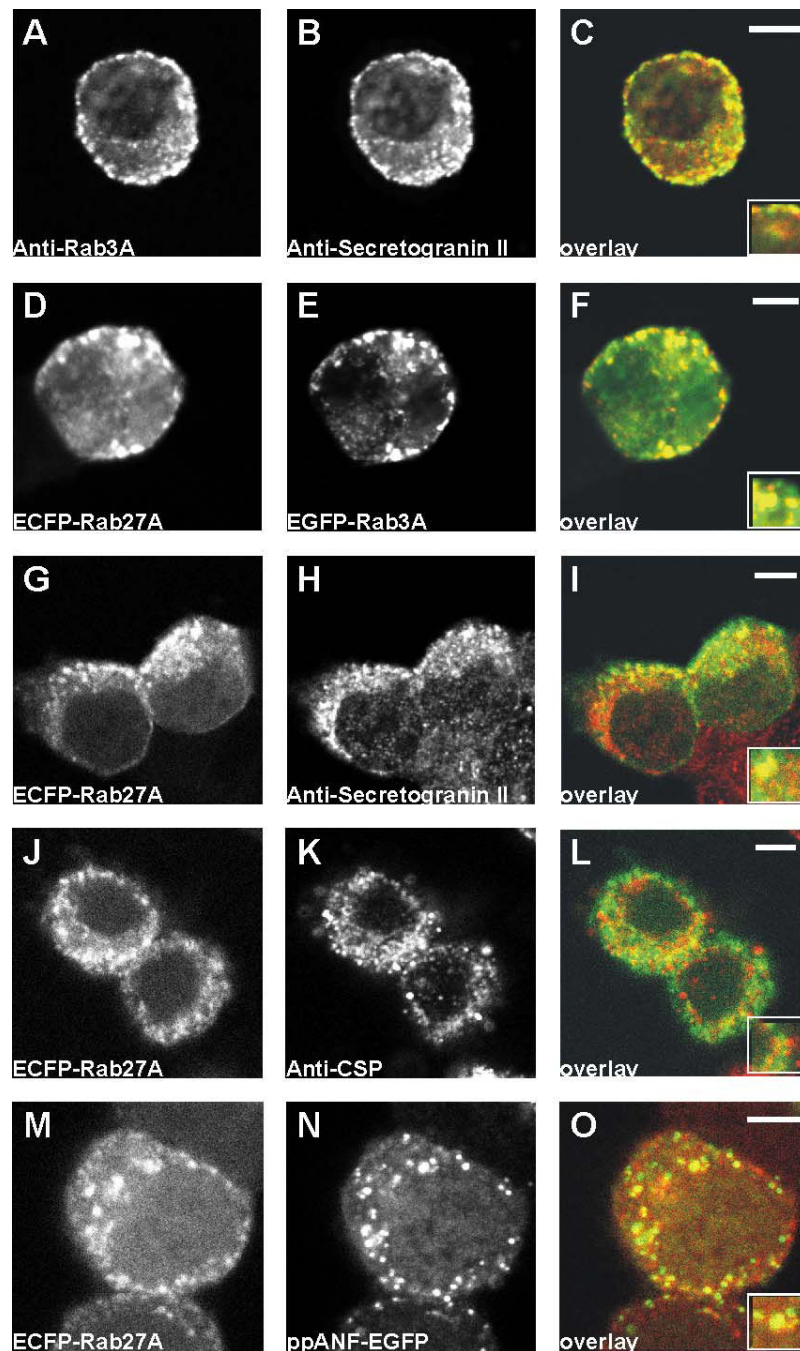


Figure 1. Recruitment of EGFP-Rab3A and EGFP-Rab27A to newly synthesised granules in PC12 cells. A-C, after fixation, cells were co-immunostained with anti-Rab3A and anti-secretogranin II (anti-SGII). D-F, cells were co-transfected with plasmids encoding ECFP-Rab27A and EGFP-Rab3A. G-I, cells were transfected with a plasmid encoding ECFP-Rab27A, and after fixation, were immunostained with anti-SGII. J-L, cells were cotransfected with plasmids encoding ECFP-Rab27A and prepro-atrial natriuretic factor-EGFP (ppANF-EGFP). In the overlay images, on the right of the figure, are composites of green, from the left image, and red from the centre image. Areas of overlap appear in yellow. The scale bars represent 4 μ m.

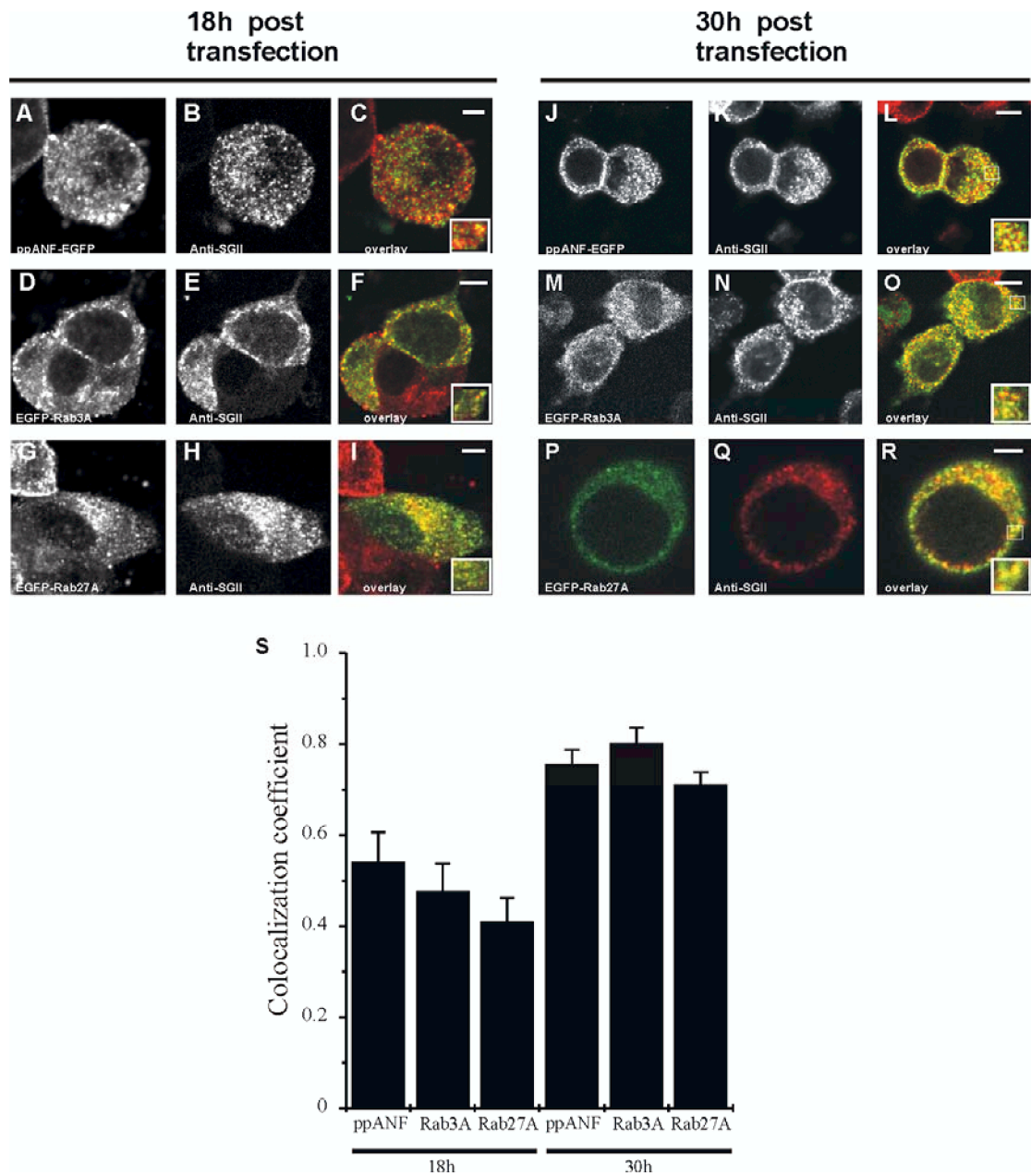


Figure 2. Improved co-localisation between ppANF-EGFP/EGFP-Rab3A/EGFP-Rab27A and secretory granules over time post-transfection. PC12 cells were transfected with ppANF-EGFP (A-C, J-L), EGFP-Rab3A (D-F, M-O) or EGFP-Rab27A (G-I, P-R), and fixed 18 hours or 30 hours following transfection as indicated. After fixation, cells were immunostained with anti-secretogranin II (anti-SGII). Images are composites of green, EGFP fluorescence, and red, anti-SGII immunofluorescence. Areas of overlap appear in yellow and increase from 18 to 30 hours post-transfection. The scale bars represent 4 μm . S, Quantification of the colocalisation of EGFP and SGII was carried out using ImageJ and the data are shown for the correlation coefficient as mean \pm SE (n=5).

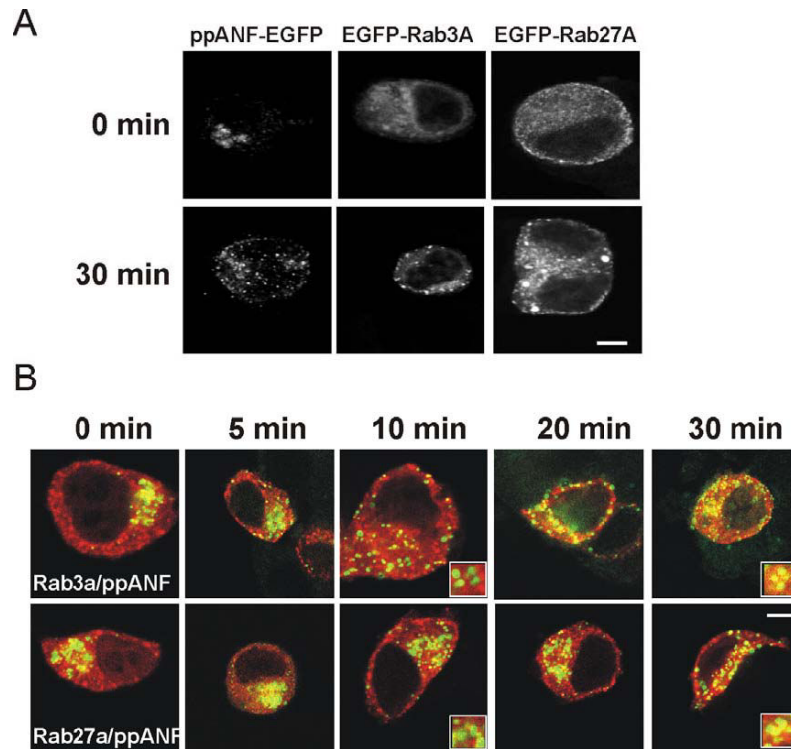


Figure 3.

Appearance of Rab3A and Rab27A on immature secretory granules during granule biogenesis and maturation. PC12 cells were transfected with ppANF-EGFP, EGFP-Rab3A, or EGFP-Rab27A (A) and cultured for 18h at 20°C to block granule budding at the TGN and then fixed (time 0) or incubated for 30 min at 37°C to allow budding of immature granules to proceed. PC12 cells were co-transfected with ppANF-EGFP and mRFP-Eab3A or mRFP-Rab27A, cultured for 18h at 20°C and then fixed at the indicated times after incubation at 37°C. The images show overlays of ppANF-EGFP fluorescence in green mRFP fluorescence in red. Expanded inserts are shown for the 10 and 30 in time points to show lack of co-localisation at 10 min and co-localisation at 30 min. The scale bars represent 4 μm .

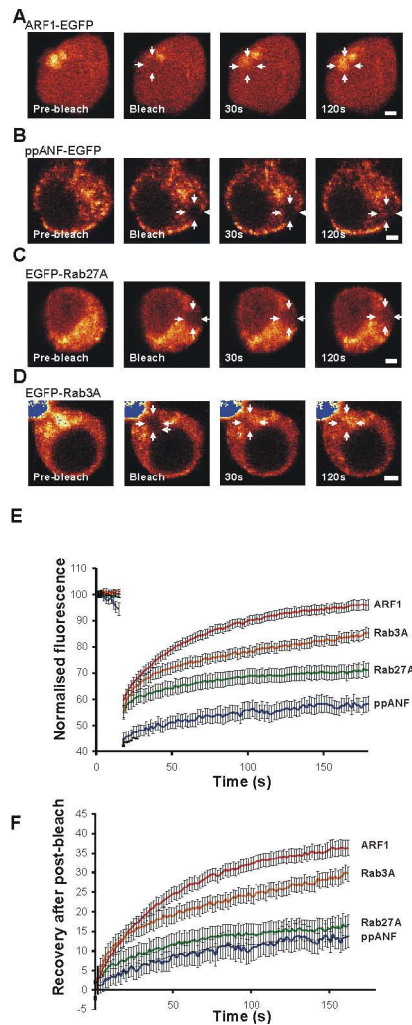


Figure 4. Dynamics of EGFP-Rab3A and EGFP-Rab27A on newly synthesised secretory granules in PC12 cells. A-D, PC12 cells were transfected to express the indicated EGFP-tagged protein and examined after 18h. Regions of interest (ROIs) in each cell were bleached with high intensity laser (see arrows), and the fluorescence recovery of these areas was followed over time. E, fluorescence in the ROI was recorded over time during low-intensity imaging. The data are shown as mean \pm SEM for 14 ARF1-EGFP, 13 ppANF-EGFP, 21 EGFP-Rab27 and 21 EGFP-Rab3A expressing cells. The data were corrected for general photobleaching for each cell at each time point and normalised by setting the initial fluorescence value for each cell to 100. F, the data were replotted with the initial post-bleach data point set to 0. The scale bars represents 2 μ m.

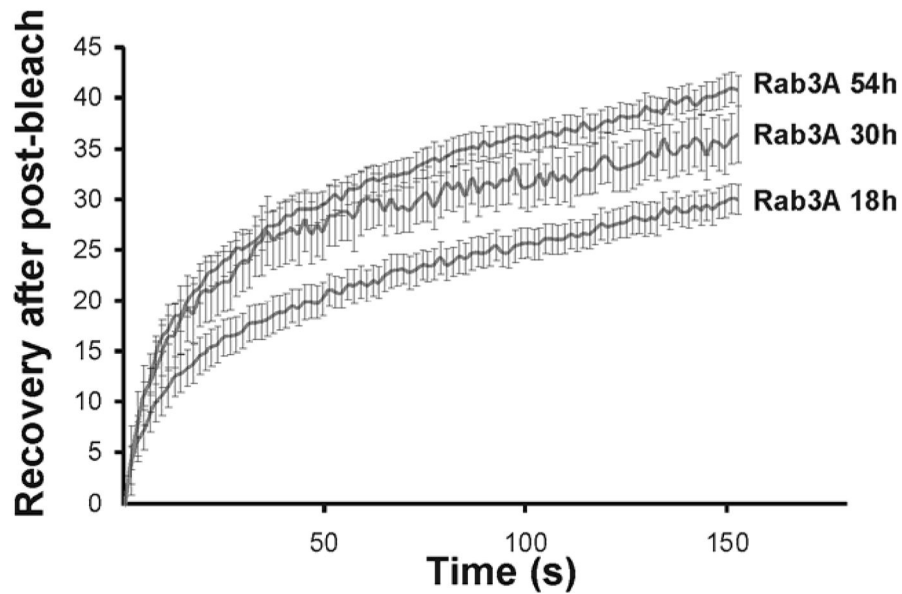


Figure 5. Dynamics of EGFP-Rab3A on newly synthesised and old secretory granules in PC12 cells. PC12 cells were transfected to express the indicated EGFP-tagged protein and examined after 18, 30 or 54h post-transfection. Regions of interest (ROIs) in each cell were bleached with high intensity laser and the fluorescence recovery of these areas was followed over time. Fluorescence in the ROI was recorded over time during low-intensity imaging. The data are shown as mean \pm SEM for 32 EGFP-Rab3A expressing cells at 18h, 10 at 30h and 27 at 54h. The data were corrected for general photo-bleaching for each cell at each time point and normalised by setting the initial fluorescence value for each cell to 100 and with the initial post-bleach datapoint set to 0.

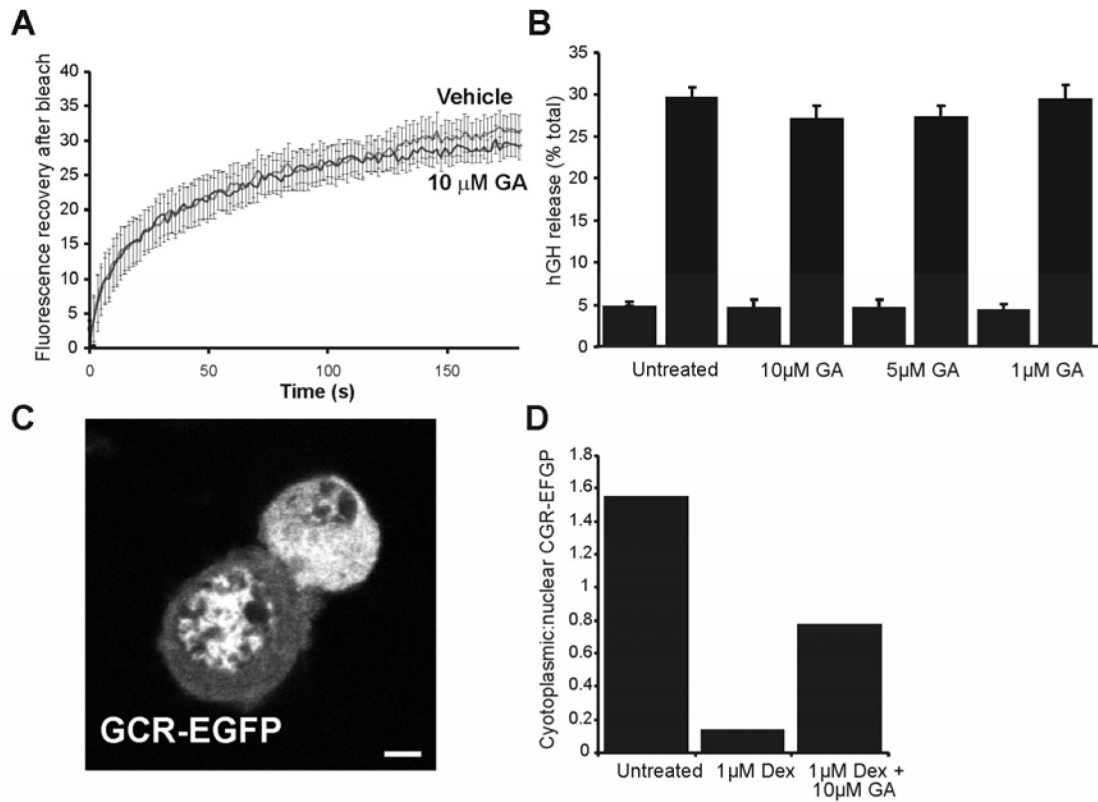


Figure 6.

Inhibition of Hsp90 does not affect EGFP-Rab3A dynamics or exocytosis in PC12 cells. A, cells were transfected with 0.5 μ g EGFP-Rab3A and at 18 hours post-transfection small regions of interest (ROIs) in each cell were bleached with high intensity laser. Fluorescence recovery was recorded over time and corrected to account for bleaching sustained during low-intensity imaging, summed, and normalised to the first datapoint post-bleach. Data are shown from control cells and cells recorded in parallel that had been treated with 10 μ M geldanamycin (GA) for 1 hour prior to bleaching (n=11 for each condition). B, secretion of exogenous human growth hormone (hGH) from cells treated with varying concentrations of GA for 1 hour prior to stimulation was assayed. Stimulated cells were exposed to 300 μ M ATP, hGH release over 15 minutes was assayed. And expressed as a percentage of total hGH C, Representative image of control cells expressing glucocorticoid receptor-EGFP (GCR-EGFP) 18h after transfection with 0.5 μ g GCR-EGFP showing two adjacent cells in which the GCR-EGFP is either predominantly cytosolic or alternatively nuclear. The scale bar represents 2 μ m. D, effect of geldanamycin on GCR-EGFP translocation to the nucleus. After transfection with GCR-EGFP, treated cells were exposed to 1 μ M dexamethasone on ice for 1 hour, or 1 μ M dexamethasone on ice for 1 hour with the addition of 10 μ M geldanamycin for the final 30 minutes. Following 20 minutes incubation at 37°C and fixation, 100 cells were scored for each condition according to the cytosolic or nuclear localisation of GCR-EGFP Data are expressed as cytoplasmic:nuclear ratios and are representative of two independent experiments.

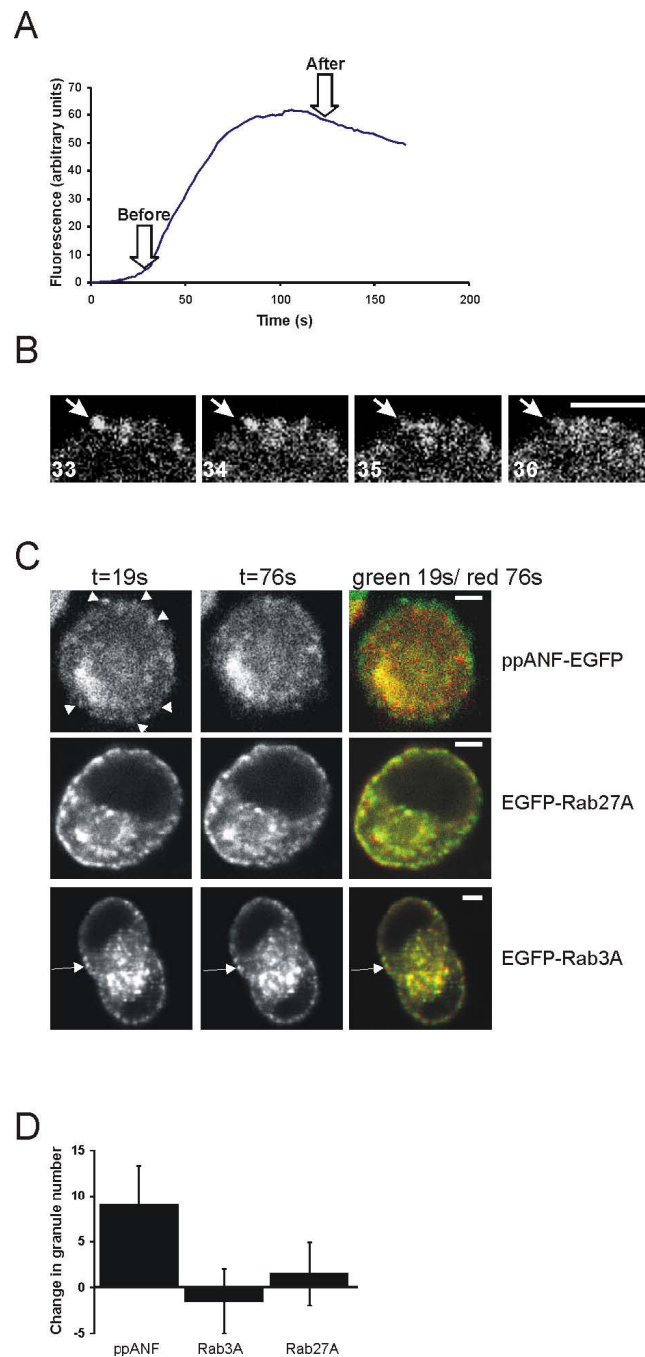


Figure 7.

Effects of expression of EGFP-Rab3A and EGFP-Rab27A on regulated secretion. In PC12 cells. Cells were transfected with the vectors indicated, as well as 0.5 μ g pXGH5 human growth hormone (hGH)-encoding vector, and pEGFP-C1 so that each transfection mix contained 1 μ g of DNA. After 48 hours, cells were washed and hGH release over 15 minutes was assayed. Cellular hGH and secreted hGH were assayed, and secreted hGH was expressed as a percentage of the total (n=6 for each condition).

Figure 7. Effect of activation of exocytosis on secretory granules labelled with EGFP-ppANF, EGFP-Rab3A or EGFP-Rab27A in live cells. Cells were transfected to express EGFP-ppANF, EGFP-Rab3A or EGFP-Rab27A and imaged 18h after transfection. Cells

showing low levels of fusion protein expression were selected for observation and stimulated by perfusion with 300 μ M ATP. A. Example of the time course of calcium changes from monitoring of X-Rhod fluorescence following ATP stimulation (n=11 cells). B. Disappearance of a ppANP-EGFP-labelled granule during stimulation. The images shown are sequential frames in which the sudden disappearance of a granule (arrow) can be observed. C. Effect of stimulation with 300 μ M ATP on secretory granules labelled with EGFP-ppANF, EGFP-Rab3A or EGFP-Rab27A as indicated. Images were taken of cells at 19s of the recording and also at 76s (after the elevation in cytosolic calcium). Overlay images are shown with t=19s in green and t=76s in red so that granules that disappear between the images are seen in green. Granules that disappeared in the ppANF-EGFP cell are indicated by arrowhead. Some granules did not disappear but moved during the recording and so appear green in the overlay and an example is indicated by the arrow in the EGFP-Rab3A transfected cell. The numbers of granules that disappear between the before and after images were identified by the comparison of images at 19 and 76s, quantified and shown as mean \pm SEM for 8 cells expressing each construct. The scale bars represent 4 μ m.